Supplementary online information

Participant ID	Transcript affected	Mutation	Melanoma-free for > 2 years prior to study	Variant Effect Predictor (VEP - Ensembl)
OX_001	P16-INK4a only	c.88delG	Yes	Frameshift variant
OX_002	P16-INK4a only	c.88delG	Yes	Frameshift variant
OX_003	P16-INK4a only	c.88delG	Yes	Frameshift variant
OX_004	Both	c.458-105A>G	Yes	Intronic variant
OX_005	Both	c.458-105A>G	Yes	Intronic variant
OX_006	Both	c.458-105A>G	Yes	Intronic variant
OX_007	P16-INK4a only	c.52_57dup	Yes	Protein altering variant
OX_008	P16-INK4a only	c.52_57dup	Yes	Protein altering variant
OX_009	Both	c.159G>A	Yes	Missense variant
OX_010	Both	c.159G>A	Yes	Missense variant
OX_011	Both	c.458-105A>G	Yes	Intronic variant
OX_012	Both	*Not tested*	Yes	*NA*
LEI_001	Both	c.225_243del19	No	Frameshift variant
LEI_002	Both	c.225_243del19	Yes	Frameshift variant
LEI_003	Both	c.225_243del19	Yes	Frameshift variant
LEI_004	Both	c.225_243del19	Yes	Frameshift variant
LEI_005	Both	c.225_243del19	Yes	Frameshift variant
LEI_006	Both	c.225_243del19	Yes	Frameshift variant
LEI_007	Both	c.225_243del19	Yes	Frameshift variant
LEI_008	Both	c.225_243del19	Yes	Frameshift variant
LEI_009	Both	c.225_243del19	Yes	Frameshift variant

LEI_010	Both	c.225_243del19	Yes	Frameshift variant
LEI_011	Both	c.67G>C	No	Missense variant
LEI_012	Both	c.225_243del19	No	Frameshift variant
LEI_013	Both	c.225_243del19	Yes	Frameshift variant
LEI_014	Both	c.225_243del19	Yes	Frameshift variant
LEI_015	Both	c.225_243del19	Yes	Frameshift variant
LEI_016	Both	c.225_243del19	Yes	Frameshift variant
LEI_017	Both	c.225_243del19	Yes	Frameshift variant
LEI_018	Both	c.225_243del19	Yes	Frameshift variant
LEI_019	Both	c.225_243del19	Yes	Frameshift variant

Supplementary table 1 List of mutations identified in carriers (annotated against CDKN2A-001 [ENST00000304494]) by targeted sequencing. The second column indicates whether the mutation maps to a region encoding just $p16^{INK4a}$ or both $p16^{INK4a}$ and $p14^{ARF}$. Participant ID is an anonymous number assigned to each case, and the prefix indicates from which cohort the patient was recruited (OX = Oxford, UK; LEI = Leiden, Netherlands).

Measure/index	Parameter	Formula or mathematical model used	Reference
iHOMA-B	Beta-cell function	Computer model available via (http://www.dtu.ox.ac.uk/homacalculator/).	(1)
iHOMA-S	Insulin sensitivity	Computer model available via (http://www.dtu.ox.ac.uk/homacalculator/).	(1)
BIGTT-AIR$_{0\text{-}30\text{-}120}$	Beta-cell function	exp[8.20 + (0.00178 * insulin$_0$) + (0.00168 * insulin$_{30}$) -(0.000383 * insulin$_{120}$) - (0.314 * glucose$_0$) - (0.109 * glucose$_{30}$) + (0.0781 * glucose$_{120}$) + (0.180 * gender (where male=0 and female=1)) - (0.032 * BMI)]	(2)
BIGTT-$S_{I\_0\text{-}30\text{-}120}$	Insulin sensitivity	exp[4.90 - (0.00402 * insulin$_0$) - (0.000556 * insulin$_{30}$) -(0.00127 * insulin$_{120}$) - (0.152 * glucose$_0$) - (0.00871 * glucose$_{30}$) - (0.0373 * glucose$_{120}$) - (0.145 * gender (where male=0 and female=1)) - (0.0376 * BMI)]	(2)
Belfiore ISI	Insulin sensitivity	2/[(0.5 * glucose$_0$ + glucose$_{60}$ + 0.5 * glucose$_{120}$)/11.36) * (0.5* insulin$_0$ + insulin$_{60}$ + 0.5* insulin$_{120}$)/638) + 1]	(3)
Matsuda ISI	Insulin Sensitivity	10 000 * √(glucose$_0$* insulin$_0$ * glucose$_{mean\text{-}OGTT}$ * insulin$_{mean\text{-}OGTT}$)	(4)
AUC	Multiple	Area under curve estimated using trapezoidal rule	(5)
Insulinogenic index	Beta-cell function	(insulin$_{30}$ – insulin$_0$)/(glucose$_{30}$ - glucose$_0$)	(6)
Disposition index	Beta-cell function	AUC$_{insulin\text{-}OGTT}$/AUC$_{glucose\text{-}OGTT}$ * Matsuda ISI	(6)
Hepatic insulin clearance	Insulin clearance	AUC$_{C\text{-}Peptide}$/AUC$_{Insulin}$	(7)
Fasting insulin clearance	Insulin clearance	C-peptide$_0$/insulin$_0$	(7)

Supplementary table 2 Definitions of physiological measurements and indices derived from the OGTT. Subscripts denote time points during the OGTT. Units are pmol/L for insulin, nmol/L for C-peptide and mmol/L for glucose, except in the case of Matsuda ISI and the disposition index, where glucose was inputted in units of mg/dL and insulin as μU/mL.

	Mutation carriers	Non-carriers	P-value
n	28	31	*NA*
BMI [cm/kg^2]	27 [19, 38]	27 [19, 37]	0.66
Age [yrs]	51 [21, 71]	52 [25, 84]	0.96
Gender [% male]	43	33	0.58
Fasting glucose [mmol/L]	5.1 [4.3, 6.3]	5.1 [3.2, 6.4]	0.92
Fasting insulin [pmol/L]	91 [15, 337]	57 [22, 150]	0.01
iHOMA-B	133 [38, 452]	99 [45, 237]	0.03
iHOMA-S	86 [18, 329]	116 [35, 236]	0.04
BIGTT-AIR [*10^3]	6.6 [0.9, 28]	3.2 [1.2, 12]	0.03
BIGTT-S	5.8 [0.4, 12.7]	7.5 [1.1, 17.8]	0.08
Belfiore ISI	0.80 [0.17, 1.35]	0.96 [0.35, 1.77]	0.03
Matsuda ISI	4.3 [0.8; 11.1]	6.1 [1.5; 20.9]	0.02
$AUC_{glucose}$	831 [563, 1449]	832 [502, 1086]	0.98
$AUC_{Insulin}$ [*10^4]	7.2 [2.4, 25]	4.9 [1.1, 15]	0.02
Insulinogenic index	205 [39, 561]	155 [53, 360]	0.10
Disposition index	2.3 [1.1, 3.8]	2.3 [1.0, 3.7]	0.92

Supplementary table 3 Comparison of OGTT-derived measures for carriers and non-carriers after exclusion of three subjects that had presented with cancer within two years prior to the study (supplementary table 1). Data are given as mean and range [min; max], and p-values are from Welch's t-test, except for gender distribution where the Chi-squared test was performed. Details on definitions of physiological measures are listed in supplementary table 2. * P-value < 0.05.

	Mutation carriers	Non-carriers	P value
n	8	8	*NA*
$AUC_{insulin}$ 0-10 min (pmol.L^{-1}.min*10^{-3})	4.8 [1.73, 13.2]	2.9 [1.84, 4.28]	0.51
$AUC_{insulin}$ 10-180 min (pmol.L^{-1}.min*10^{-3})	35.5 [13.7, 94.9]	16.9 [12.5, 22.2]	0.16
$AUC_{C\text{-}peptide}$ 0-10 min (pmol.L^{-1}.min*10^{-3})	15.1 [9.1, 31.9]	11.7 [5.5, 14.5]	0.96
$AUC_{C\text{-}peptide}$ 10-180 min (pmol.L^{-1}.min*10^{-3})	198 [103, 364]	152 [101, 186]	1.00
Net IVGTT insulin secretion 0-10 min (pmol.L^{-1})	0.56 [0.29, 0.84]	0.50 [0.10, 1.04]	0.65
Net IVGTT insulin secretion 10-180 min (pmol.L^{-1})	4.2 [1.20, 11.8]	2.8 [1.10, 4.98]	0.65
Insulin sensitivity, S_I (min^{-1}.$pmol^{-1}$.L)	0.72 [0.19, 1.28]	0.68 [0.30, 0.95]	0.72
Disposition index [*10^{-3}]	2.4 [1.14, 4.44]	1.9 [0.77, 3.40]	0.51
C-peptide disposition index	8.9 [3.45, 12.6]	7.8 [4.00, 13.7]	0.80
Fractional hepatic insulin throughput	0.53 [0.34, 1.12]	0.41 [0.26, 0.74]	0.23
Plasma insulin elimination rate (min^{-1})	0.098 [0.025, 0.207]	0.095 [0.042, 0.235]	0.72

Supplementary table 4 IVGTT-derived measures of β-cell function, insulin sensitivity and hepatic clearance. Data are given as mean and range [min; max]. All p-values are based on Mann-Whitney U test.

Supplementary figure legends

Supplementary figure 1 Serum glucose (*left panel*) and insulin (*right panel*) levels during a 120-min OGTT in twenty-six cases with *CDKN2A* loss-of-function mutations affecting both $p16^{INK4a}$ and $p14^{ARF}$ (*black triangles, dotted line*), five cases with *CDKN2A* loss-of-function mutations affecting $p16^{INK4a}$ exclusively (*black squares, solid line*), and thirty-one BMI-, age-, and gender-matched controls (*white circles, dashed line*). Data shown as mean +/- SEM.

Supplementary figure 2 Serum glucose (*left panel*) and insulin (*right panel*) levels during a 180-min IVGTT in eight carriers (*pink circles*) and eight BMI- ($p = 0.72$), age- ($p = 0.96$), and gender-matched ($p = 0.50$) controls (*blue squares*). Data shown as mean +/- SEM.

Supplementary figure 3 Immunofluorescence staining of p16INK4a (Abcam, ab81278; recognizing isoform 1 of the protein) in the human beta-cell line, EndoC-bH1. In siRNA-mediated knockdown experiments, expression of p16INK4a protein was visibly down-regulated (*bottom panel*) as compared with control cells (*top panel*). Cell nuclei were stained using NucRed Dead 647 (Life Technologies). Images were taken on a BioRad Radiance 2100 confocal microscope with a 60X 1.0 N.A. objective, and the same laser settings and intensities were used across samples. Scale bar, 20 μm.

Supplementary figure 4 Gene expression profiles of critical cell-cycle regulators after silencing of *CDKN2A* in the human β-cell line, EndoC-bH1. Knockdown experiments were performed as described for figure 2. Relative gene expression of *CDK4* (*top left*), *CDK6* (*top right*), *CDKN2A* (*bottom left*) and *CDKN2B* (*bottom right*) corrected for expression of two housekeepers using the delta-delta Ct method, and normalized to non-targeting control. As shown, we observed efficient knockdown of CDKN2A with no off-target effect on the *CDKN2B* gene. Bars represent means for n = 4-5 and error bars are SEM.

Supplementary figure 5 Insulin content normalized to cell-count following *CDKN2A* knockdown. After static insulin secretion assays, cells were counted and insulin contents extracted as described in figure 2. Using these data, the insulin content relative to the number of cells per well was calculated as the ratio between these two numbers, and normalized to scrambled control. Bars represent means for the aggregate of basal and high glucose measurements for n = 16, and error bars are SEM.

Supplementary figure 6 PKA activity in the EndoC-bH1 cell line following *CDKN2A* knockdown. 96 h after treatment with non-targeting ("scrambled"; *blue bar*) or *CDKN2A* (*red bar*) siRNAs, cells were harvested and PKA activity measured on sample input normalized to cell numbers. Substrate conversion rates were calculated as the ratio of non-phosphorylated to total peptide using fluorescence intensities quantified with standard software on the ChemiDoc MP system. Data shown as mean +/- SEM for three independent replicates.

Supplementary figure 7 Outline of two non-mutually exclusive mechanisms compatible with the phenotype of *CDKN2A* mutations-carriers. According to model 1 (*left*), a primary reduction in insulin sensitivity leads to a compensatory increase in insulin secretion to maintain glucose homeostasis. The effect of *CDKN2A*-loss would therefore be in non-beta cell tissues, such as liver. Model 2 (*right*), in contrast, represent the alternative scenario: chronically elevated insulin levels due to β-cell hypersecretion drives a progressive decrease in insulin receptors and insulin signalling through homologous desensitization (8). In this case, the primary effect of *CDKN2A* loss is on the pancreatic beta-cell, but the mechanism ultimately manifests as impaired insulin sensitivity and reduced insulin clearance. As discussed in the main text, it is likely that a combination of the two models contributes to both beta-cell hypersecretion and primary insulin resistance.

Supplementary figure 8 Screenshot from the Human Islet Regulome Browser (9) showing annotations of chromatin state, transcription factor binding and variant association with type 2 diabetes at the *CDKN2A/B locus*. The genomic binding sites of islet transcription factors (PDX1, NKX2.2, FOXA2, NKX6.1, MAFB) are indicated by lines connected to the respective proteins. A Manhattan plot above shows log(p-values) of association with type 2 diabetes for variants in the MAGIC (*blue*) and DIAGRAM (*red*) datasets (10, 11). Lead variants tagging the two genome-wide association signals located downstream of *CDKN2B-AS1* are shown. Fine-mapping efforts have since publication of the islet regulome narrowed down the number of potential causative variants to credible sets of five and six variants (Gaulton et al, (2015) Nature Genetics, *in press*). Both of these sets contain variants that directly overlap a FOXA2 binding site.

Supplementary references

1 Matthews, D.R., *et al.* (1985) Homeostasis model assessment: insulin resistance and beta-cell function from fasting plasma glucose and insulin concentrations in man. *Diabetologia* 28, 412-419
2 Hansen, T., *et al.* (2007) The BIGTT test: a novel test for simultaneous measurement of pancreatic beta-cell function, insulin sensitivity, and glucose tolerance. *Diabetes Care* 30, 257-262
3 Belfiore, F., *et al.* (1998) Insulin sensitivity indices calculated from basal and OGTT-induced insulin, glucose, and FFA levels. *Mol Genet Metab* 63, 134-141
4 Matsuda, M. and DeFronzo, R.A. (1999) Insulin sensitivity indices obtained from oral glucose tolerance testing: comparison with the euglycemic insulin clamp. *Diabetes Care* 22, 1462-1470
5 Pacini, G. and Mari, A. (2003) Methods for clinical assessment of insulin sensitivity and beta-cell function. *Best Pract Res Clin Endocrinol Metab* 17, 305-322
6 Phillips, D.I., *et al.* (1994) Understanding oral glucose tolerance: comparison of glucose or insulin measurements during the oral glucose tolerance test with specific measurements of insulin resistance and insulin secretion. *Diabet Med* 11, 286-292
7 Herzberg-Schafer, S.A., *et al.* (2010) Evaluation of fasting state-/oral glucose tolerance test-derived measures of insulin release for the detection of genetically impaired beta-cell function. *PLoS One* 5, e14194
8 Shanik, M.H., *et al.* (2008) Insulin resistance and hyperinsulinemia: is hyperinsulinemia the cart or the horse? *Diabetes Care* 31 Suppl 2, S262-268
9 Pasquali, L., *et al.* (2014) Pancreatic islet enhancer clusters enriched in type 2 diabetes risk-associated variants. *Nat Genet* 46, 136-143
10 Morris, A.P., *et al.* (2012) Large-scale association analysis provides insights into the genetic architecture and pathophysiology of type 2 diabetes. *Nat Genet* 44, 981-990
11 Voight, B.F., *et al.* (2010) Twelve type 2 diabetes susceptibility loci identified through large-scale association analysis. *Nat Genet* 42, 579-589

Supplementary figure 1

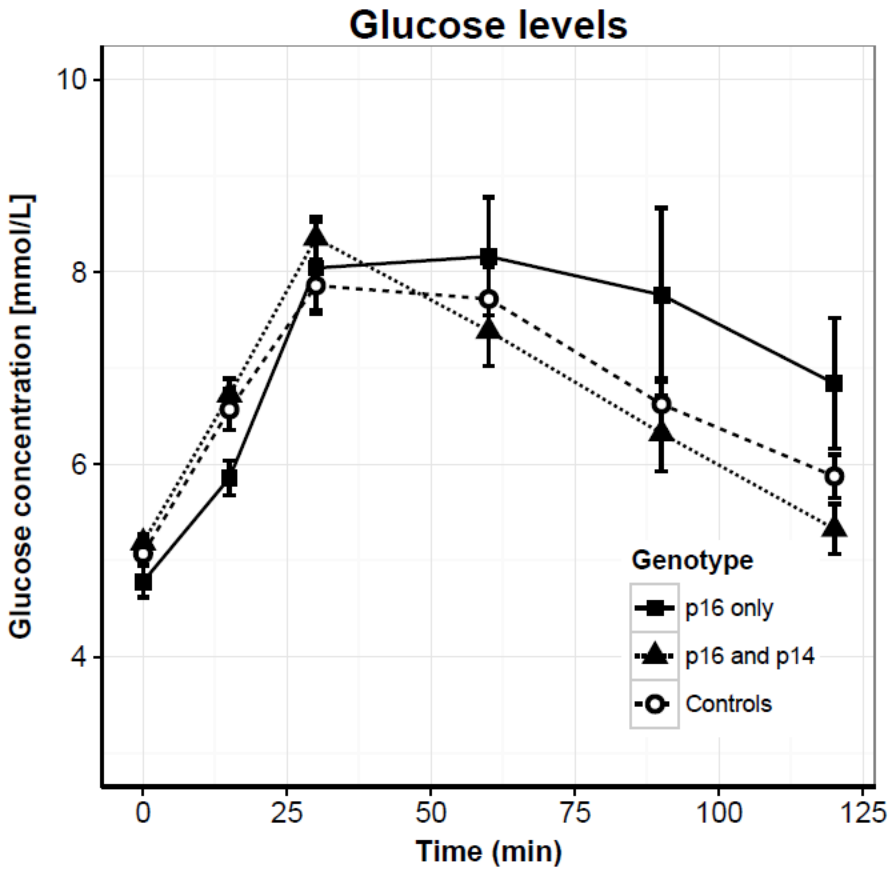

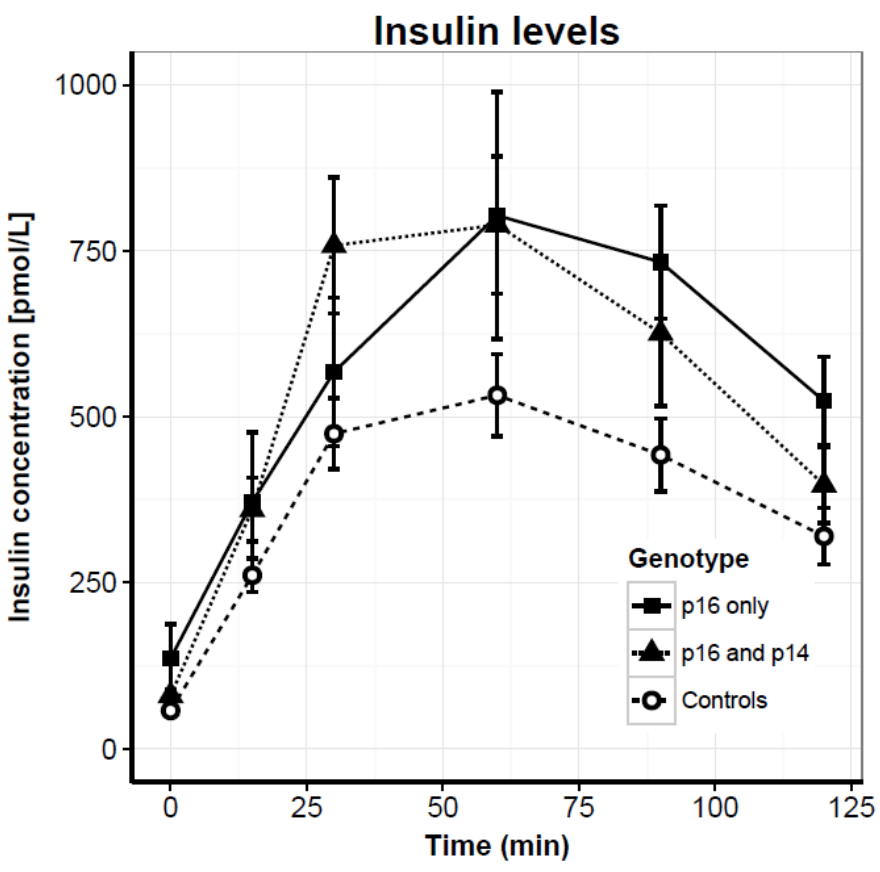

Supplementary figure 2

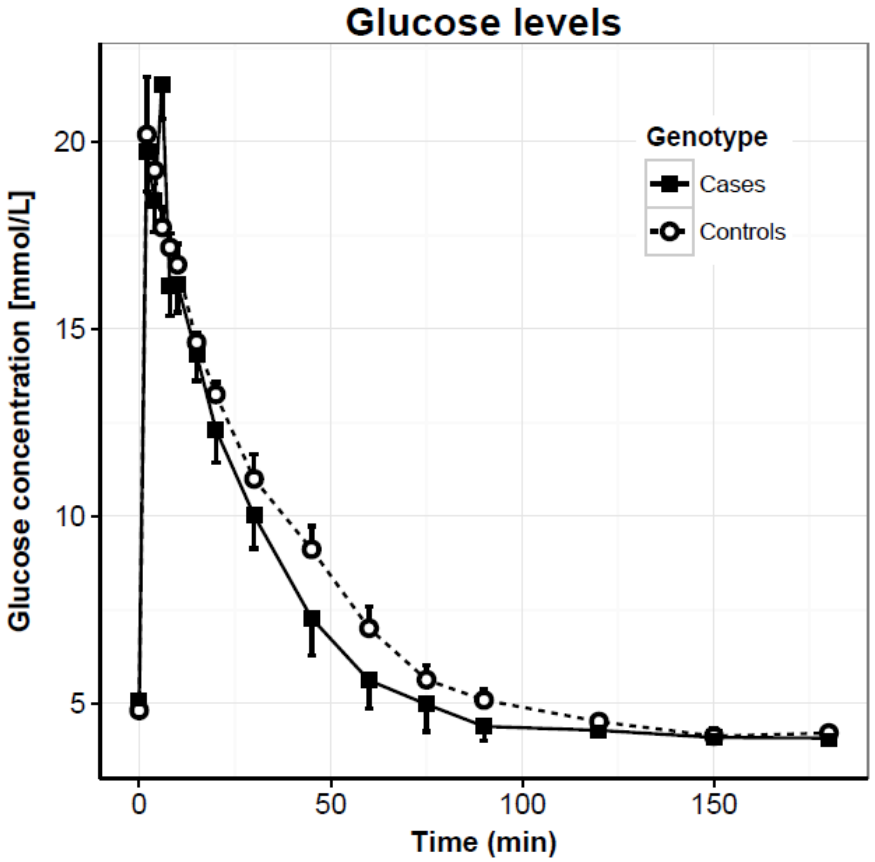

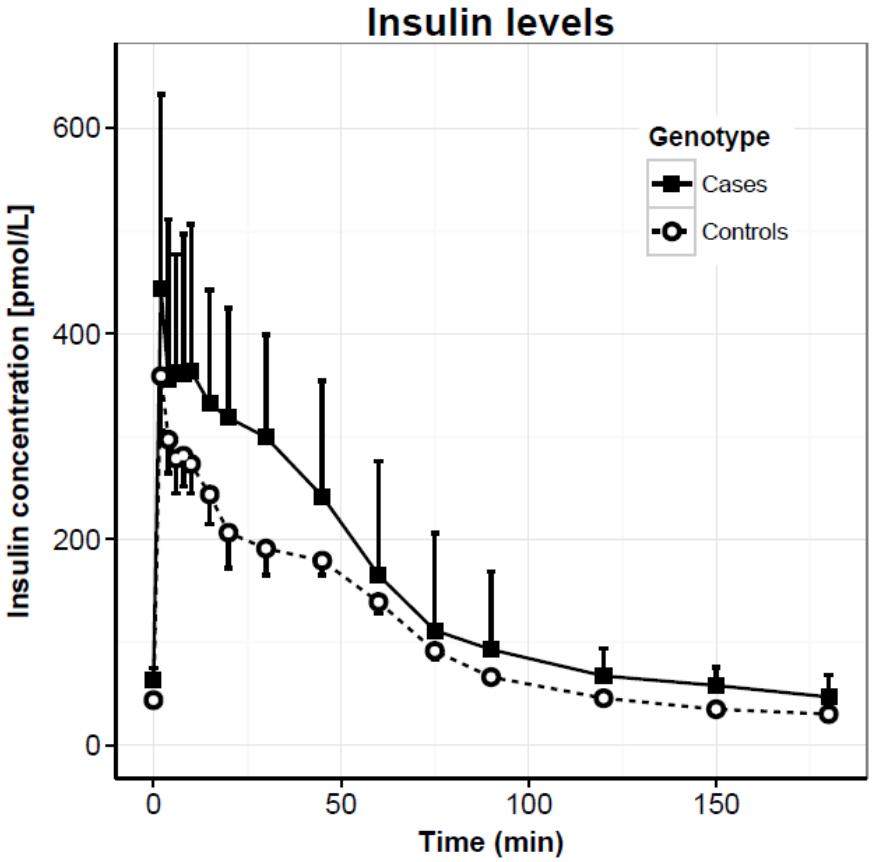

Supplementary figure 3

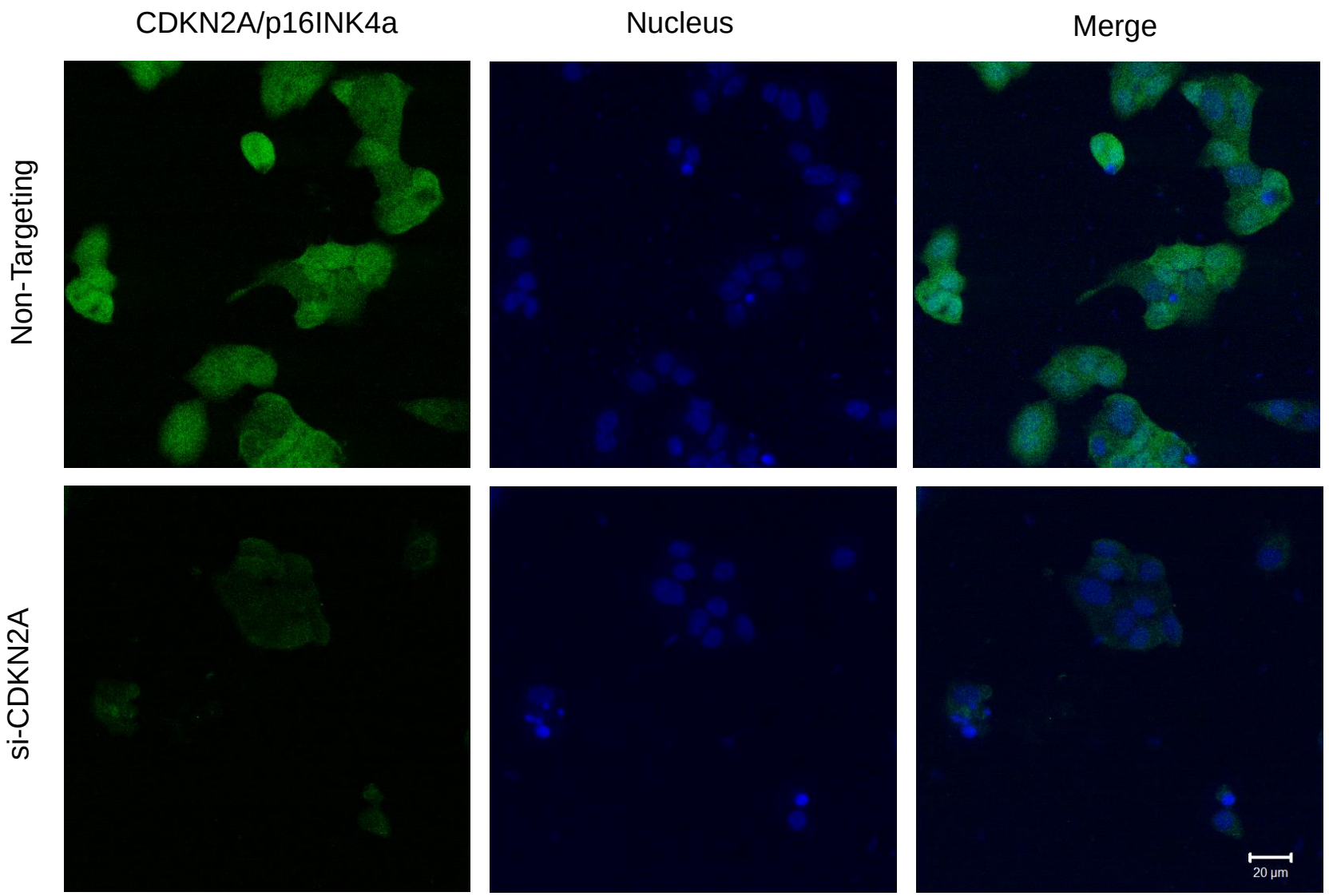

Supplementary figure 4

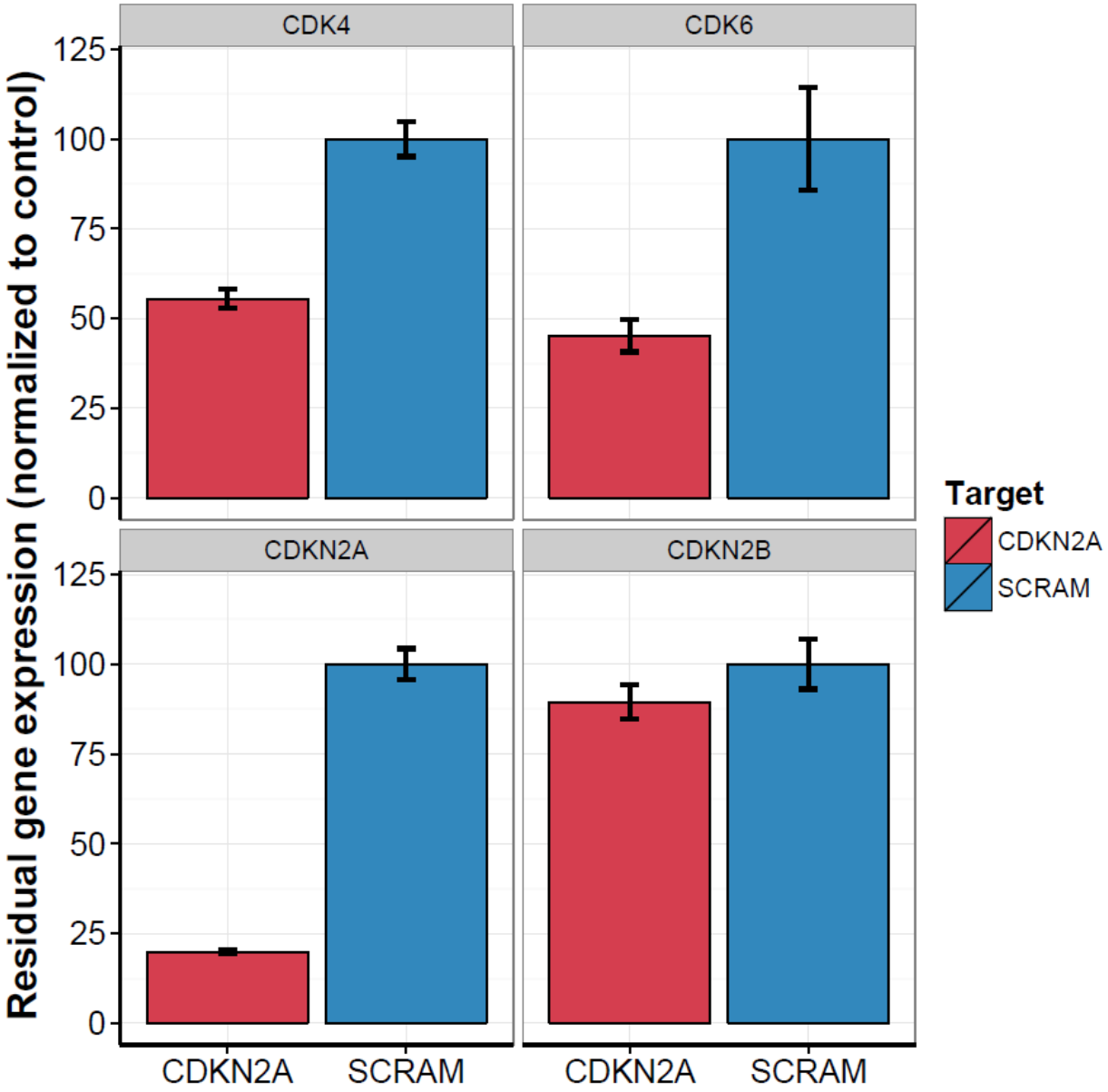

Supplementary figure 5

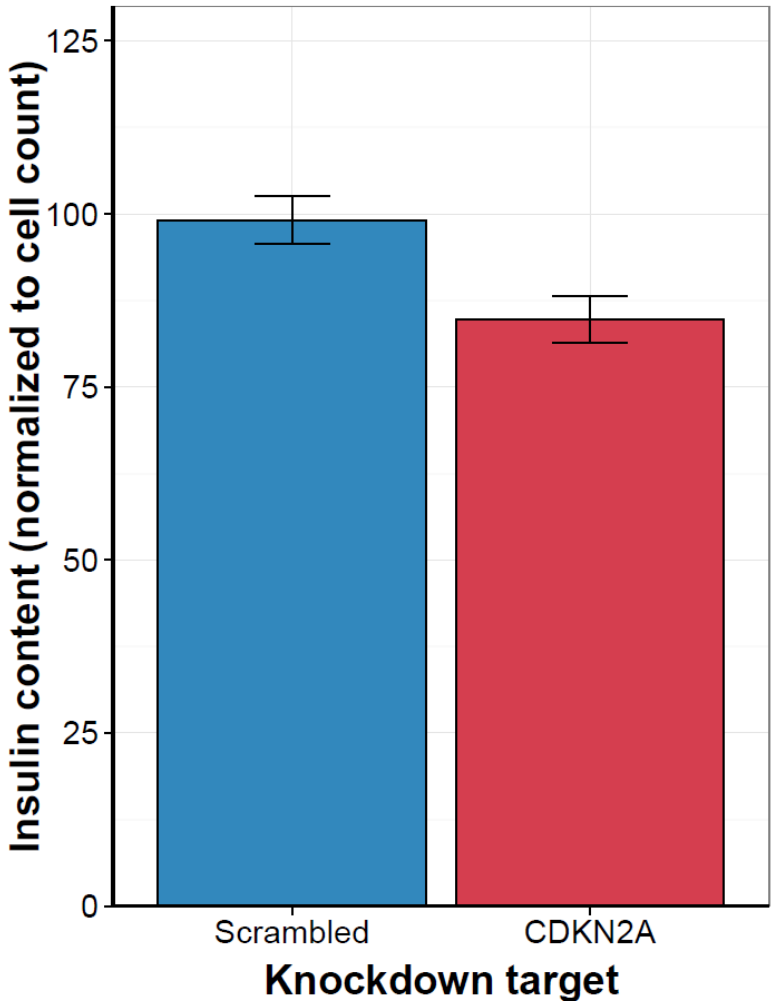

Supplementary figure 6

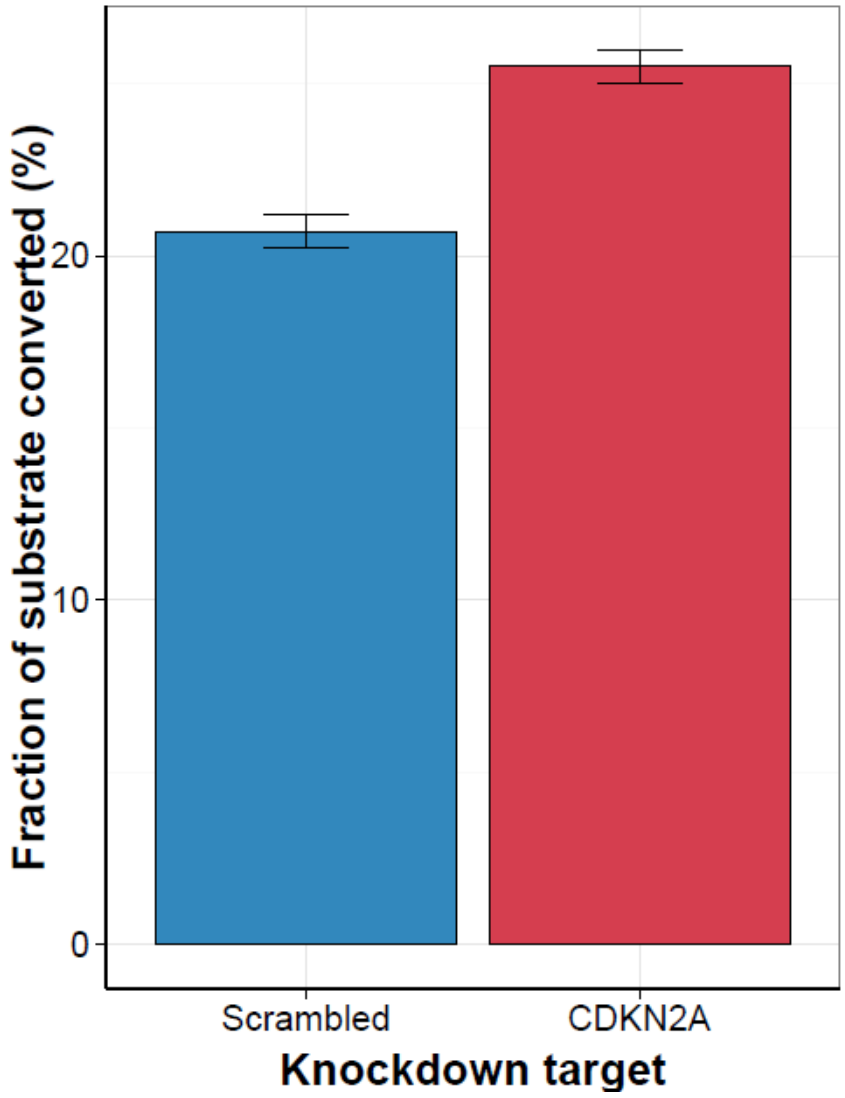

Supplementary figure 7

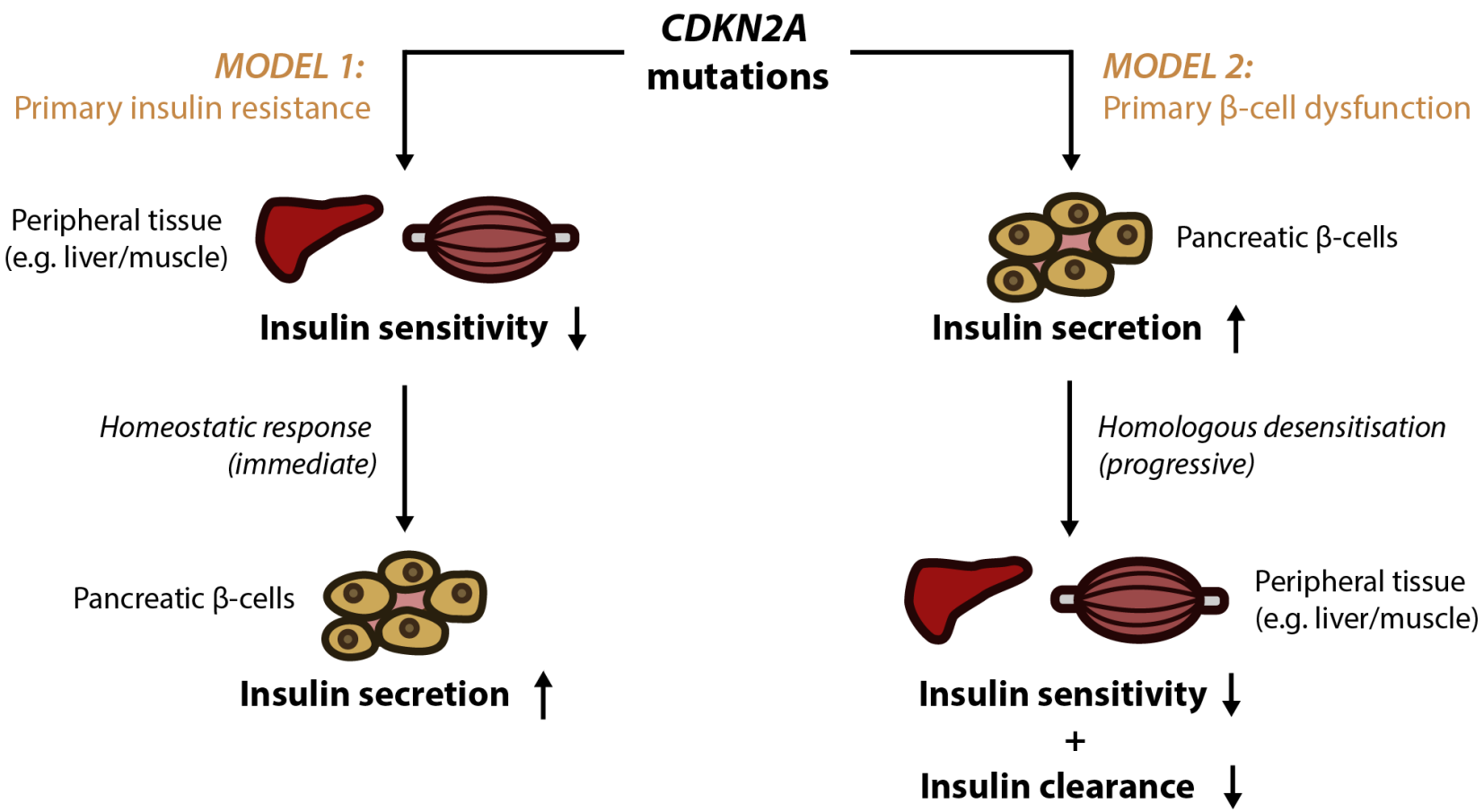

Supplementary figure 8